Electrical levels of dislocation networks in p- and n-type Si

I Isakov [a]*, A Bondarenko [a], O Vyvenko [a], V Vdovin [a], E Ubyivovk [a] and O Kononchuk [b]

[a] V.A. Fok Institute of Physics, St. Petersburg State University, 198504 St. Petersburg, Russia
[b] SOITEC, Parc des Fontaines, F-38560, Bernin, France
*Corresponding author. E-mail: isakov@nano.spbu.ru

Abstract. The results of deep level transient spectroscopy (DLTS) and minority carrier transient spectroscopy (MCTS) investigations on directly bonded n- and p-type silicon wafers with small twist misorientation angles ranging from 1 to 5 degrees are presented and discussed. Both shallow and deep levels in the upper half of a band gap are found and a good correspondence between the DLTS and MCTS data on n- and p-type samples was established. The dependence of DLTS-peak magnitude on twist and tilt misorientation angles (density of dislocations) was investigated and the origin of different levels is suggested.

1. Introduction

Dislocation networks (DN) obtained by the direct wafer bonding (WB) technique are perfect model objects for deeper understanding of the electronic properties of dislocations in silicon [1,2] since this technology allows one to create samples with DN of well controlled structure at depths well suited for space charge spectroscopy measurements and transmission electron microscopy (TEM) imaging. Such investigation might prompt development of models for dislocation-related phenomena that are attracting interest due to their importance for future application in dislocation related luminescence [2] and conductivity enhancement along DN in Si DN [3].

DLTS measurement of WB DNs were carried out mostly on p-type Si and only levels in the lower half of band gap were examined. In this work we present the result of a combined study of the dislocation-related electrical levels in the upper half of the band gap by means of DLTS measurements on n-type Si WB or by MCTS measurements on p-type Si and of the dislocation structure by TEM.

2. Experimental Method

A set of p-type (boron doped) and n-type (phosphorus doped) Czochralski grown Si wafers with initial doping concentration of 10^{15} and 10^{14} cm^{-3} respectively and (100) surface orientation were bonded hydrophilically with twist misorientation angles (TMA) of approximately 1° — 5°, and unavoidable tilt angles of about 0.5°. The wafers were thinned in order to have the DN depth of 200 nm from the surface. Details on the bonding procedure can be found elsewhere [2]. Semitransparent titanium (gold) contacts for p- (n-) type silicon with a thickness of about 20 nm were sputtered on top of the wafers to prepare Shottky diodes.

DLTS and MCTS measurements were conducted using a SULA Tech. Inc. instrument. Sample temperature was varied from 20 to 300 K by means of a Janis closed cycle helium cryostat. All measurements were carried out at the same initial conditions. The reverse bias voltage was kept –1 V. The filling pulse voltage for majority carrier excitation was +2 V with a duration of 200 μsec, time

period between pulses was 50 ms, and the rate windows ranged from 0.2 ms to 20 ms. A light emitting diode with a wavelength of 890 nm was used to provide optical excitation of minority carriers. In order to examine the influence of the electrical field on the level position the applied reverse bias voltage was varying from 0 to 12 V. To retrieve the concentration of levels from data we used the following formula:

$$N_{ds} = \frac{\left(A\varepsilon\varepsilon_0\right)^2}{x_d} eN_d \frac{\Delta C}{C_3}, \quad (1)$$

where A is contact area, x_d is depth from the surface, N_d is doping concentration, C is capacitance, ΔC is the signal magnitude of DLTS (MCTS) peak.

TEM analysis was performed using a Zeiss Libra 200FE transmission electron microscope at different diffraction conditions. The electron beam acceleration voltage was 200 kV.

3. Results and discussion

3.1. Microstructure

TEM micrographs revealed regular screw dislocation networks compensating the twist, interrupted by dark lines related to tilt (figure 1a, b, c, right column). For low-angle samples edge dislocations are presented by zigzag lines of 60° dislocations (figure 1a right) described in the literature [4]. High-angle samples exhibit Moiré patterns which result in visually reducing the distance between dislocations by a factor of two (figure 1b right). We have extracted the twist and tilt angles between bonded wafers from measured distance between dislocations and using Frank's formula for fcc crystals

$$d \cong a / \sqrt{2} \sin\theta \quad (2)$$

(where d is a distance between dislocations, $a = 0.543$ nm is a lattice constant for Si, and θ is a misorientation angle). The summary of structural properties for all the samples is given in Table 1. It should be noted that the tilt in these samples was in the range 0.4° — 0.9°. Some pairs of p- and n-type samples, e.g. n-3.5°/0.6° and p-3.7°/0.7°, n-5.0°/0.45° and p-4.9°/0.9°, have close twist and tilt angle values and thus could be compared by charge spectroscopy techniques.

All the samples but one have 60°-dislocation families parallel to one of the component of screw dislocations square network (figure 1 right). Only the sample p-3.0°/0.7° has an edge dislocation line at about 30° (or 60°) to one component of the screw dislocation array.

Table 1. Summary data derived from TEM observations: *dtw* and *dti* — average distances between twist and tilt dislocations respectively. *Dsc* and *Ded* are the line densities of screw and edge dislocations. α_{TW} and α_{TI} are the twist and tilt misorientation angles calculated using Frank's formula (2). The labels are given with respect to the twist/tilt misorientation angles.

Sample label	α_{TW}, °	*dtw*, nm	Dsc, 10^6 cm^{-1}	α_{TI}, °	*dti*, nm	Ded, 10^6 cm^{-1}
"n-0.9°/0.55°"	0.9±0.1	23±3	0.43	0.55±0.15	39±9	0.26
"n-1.5°/0.55°"	1.7±0.1	12.9±0.7	0.78	0.55±0.1	38±7	0.26
"n-3.5°/0.6°"	3.5±0.2	6.3±0.3	1.6	0.6±0.1	35±7	0.29
"n-5.0°/0.45°"	5.0±0.4	4.5±0.4	2.2	0.45±0.1	46±6	0.22
"n-5.7°/0.5°"	5.7±0.2	3.8±0.2	2.6	0.5±0.1	40±4	0.25
"p-2.3°/0.7°"	2.3±0.1	9.6±0.3	1.0	0.7±0.1	32±5	0.31
"p-3.0°/0.7°"	3.0±0.1	7.4±0.2	1.4	0.7±0.05	30±4	0.33
"p-3.7°/0.7°"	3.7±0.4	6.0±0.6	1.7	0.7±0.05	32±3	0.31
"p-4.9°/0.9°"	4.9±0.5	4.6±0.4	2.2	0.9±0.05	25±2	0.4

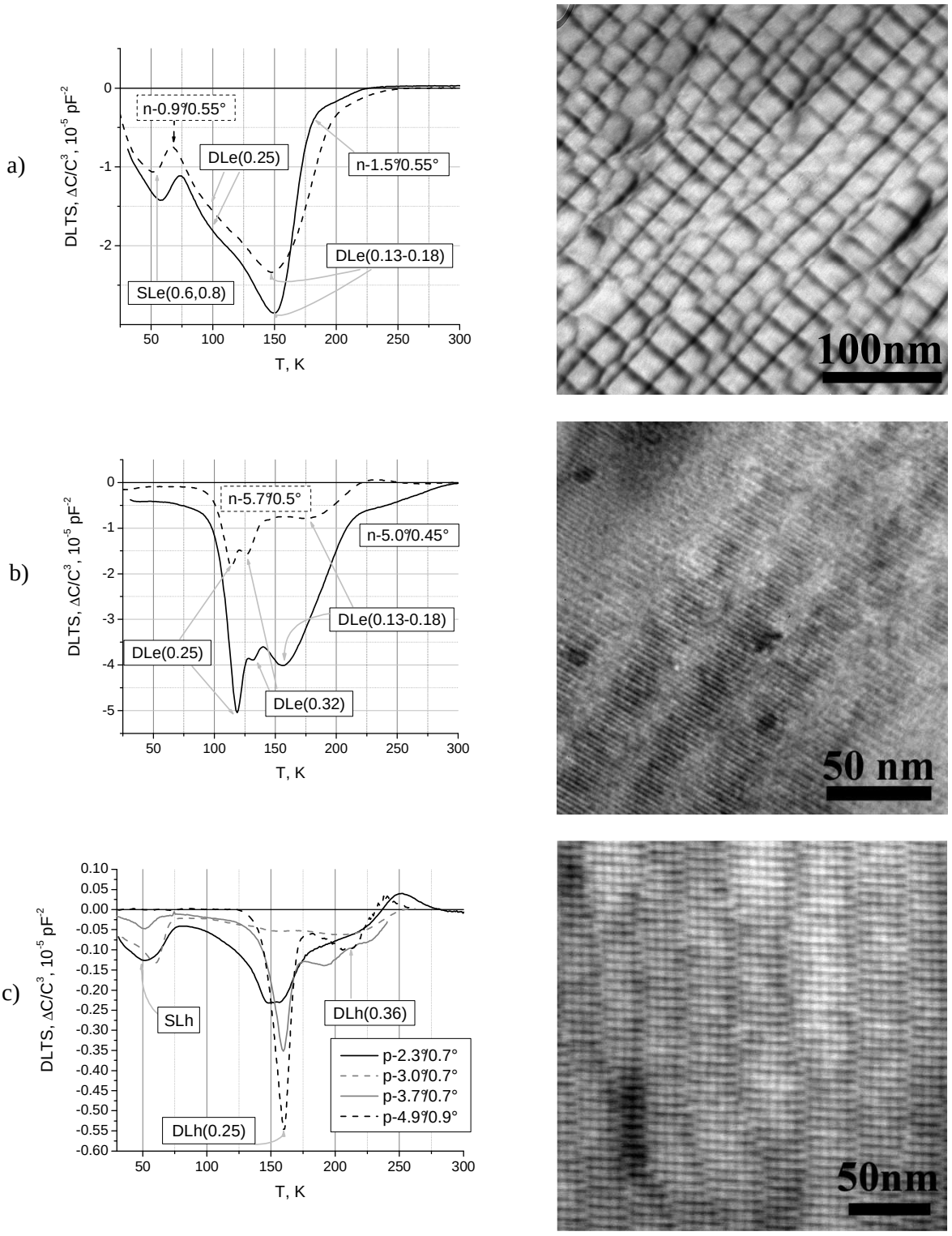

Figure 1. DLTS-spectra (left) for different subsets of samples. a) ""n-0.9°/0.55°"" ,"n-1.5°/0.55°" b) "n-5.0°/0.45°", "n-5.7°/0.5°" c) all the p-type samples. Corresponding TEM-images (right) of a) ""n-0.9°/0.55°"", b) "n-5.0°/0.45°", c) "p-3.7°/0.7°". DLTS conditions: $V_{rev} = -1V;\ V_{pulse} = +2V;\ t_{pulse} = 200\mu s;\ T_{period} = 50ms$, emission rate window $20ms$.

3.2. Space charge spectroscopy

Typical DLTS-spectra obtained on diverse samples are presented in figure 1 (left column). A +2 V pulse was used as it was determined to saturate all the levels. Summarized details of the DLTS and MCTS measurements are shown on the Arrhenius plots in figure 2 and in Table 2. In the present work for the first time we have observed levels in the upper-part of the band gap corresponding to dislocation network in WB Si. The overview of these levels is presented below.

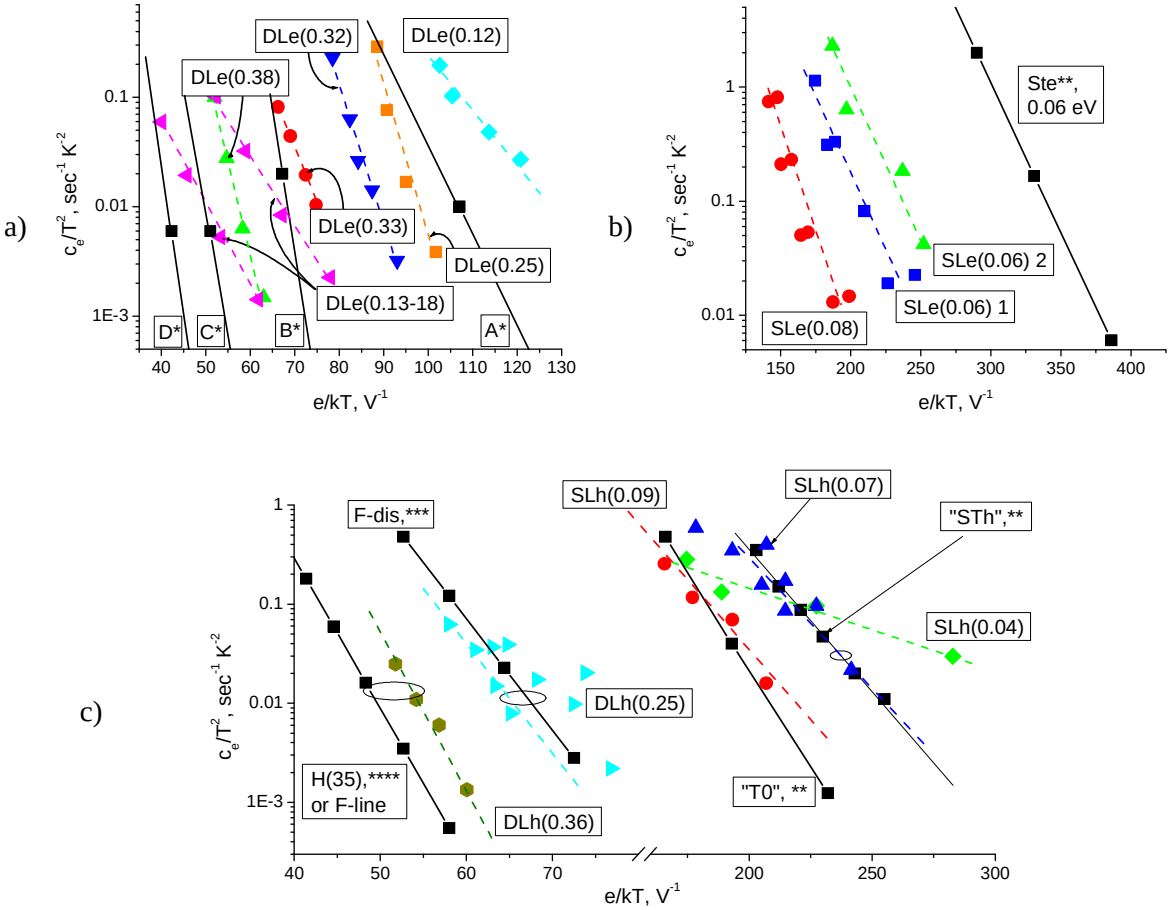

Figure 2. Arrhenius plots derived from DLTS and MCTS measurements for electron and hole traps. a) deep electron traps; b) shallow electron traps; c) hole traps. The dashed (colour) lines represent linear fitting of our data, solid black lines and black squares represent data reported in literature:
* – Omling [5]; ** – Castaldini et al. [6]; *** – Vyvenko et al. [7], **** – Kimerling and Patel [8].
Arrhenius plots attributed by us to the same level are joined by black ovals. See discussion in the text.

Table 2. The list of levels and samples with corresponding literature data (** – Castaldini et al. [6]; **** – Kimerling and Patel [8])

Level family	Level label (activation energy)	Cross-section, cm^2	Samples observed	Level family	Level label (activation energy)	Cross-section, cm^2	Samples observed
SLe	SLe(0.06) 1,	10^{-17}	n-0.9°/0.55°	SLh	SLh(0.07)/ STh** [6]	10^{-16}–10^{-17}	p-3.7°/0.7°, n-3.5°/0.6°, n-1.5°/0.55°
	SLe(0.06) 2	10^{-18}	p-3.0°/0.7°		SLh(0.09)/ T0** [6]	10^{-14}–10^{-15}	p-3.0°/0.7°
	SLe(0.08)	10^{-15}–10^{-16}	n-1.5°/0.55°, n-3.5°/0.6°, p-3.7°/0.7°		SLh(0.05)	10^{-17}–10^{-18}	p-2.3°/0.7°
DLe narrow	DLe(0.25)	10^{-12}–10^{-13}	n-0.9°/0.55°, n-1.5°/0.55°, n-3.5°/0.6°, p-3.7°/0.7°, n-5.0°/0.45°, n-5.7°/0.5°	DLh	DLh(0.25)	10^{-13}–10^{-14}	p-2.3°/0.7°, p-3.7°/0.7°, p-4.9°/0.9°, p-3.0°/0.7°
	DLe(0.33)	$5\cdot10^{-14}$	n-3.5°/0.6°, p-3.7°/0.7°, p-3.0°/0.7°		DLh(0.15)	10^{-18}	n-0.9°/0.55°, n-1.5°/0.55°, n-5.0°/0.45°, n-5.7°/0.5°
	DLe(0.38)	10^{-15}	n-3.5°/0.6°				
	DLe(0.32)		n-5.0°/0.45°, n-5.7°/0.5°		DLh(0.36)/ F-line,****[8]	10^{-13}	p-3.0°/0.7°, p-2.3°/0.7°, p-3.7°/0.7°, p-4.9°/0.9°, n-3.5°/0.6°
DLe wide	DLe(0.12)	$5\cdot10^{-12}$–$5\cdot10^{-13}$	p-3.0°/0.7°				
	DLe(0.13-0.18)	10^{-19}–10^{-21}	n-0.9°/0.55°, n-1.5°/0.55°, n-3.5°/0.6°, n-5.0°/0.45°, n-5.7°/0.5°				

3.2.1. Levels in the upper half of the band gap in Si

Shallow electron traps (SLe) were found in some n- and p-type samples. Shallow 1D bands have been predicted near both conduction and valence bands in the dislocated semiconductors [9]. Shallow electron traps were first observed in [6] in plastically deformed Si (figure 2b, "Ste**"). The activation energies of SLe(0.06) 1 and SLe(0.06) 2 coincide well with this shallow electron trap ($E_{Ste**} = 0.06eV$), however, the cross-sections differ significantly from those reported previously (figure 2b). The activation energies measured in the experiment could represent a difference between certain trap energy and the bottom of 1D-band ($E_C - E_{D1e}$) as was proposed by Kveder *et al*. in [10]. This is an unlikely scenario since in that case the level corresponding to transition between trap and conduction band with $E_t = 0.06(0.08) + E_{D1e}$ should be present in the DLTS-spectrum, but it is absent.

Hence the transition SLe(0.08;0.06) should arise between the trap level (or 1D-band) and the conduction band directly.

Shallow electron trap concentration as a function of TMA is presented in figure 3a. The concentration of SLe-level grows with TMA from 1° to 3.5° and then rapidly decreases to zero. This dependence might be explained as a result of the changes of the dislocation deformation potential caused by increasing interaction of the strain field of screw dislocations.

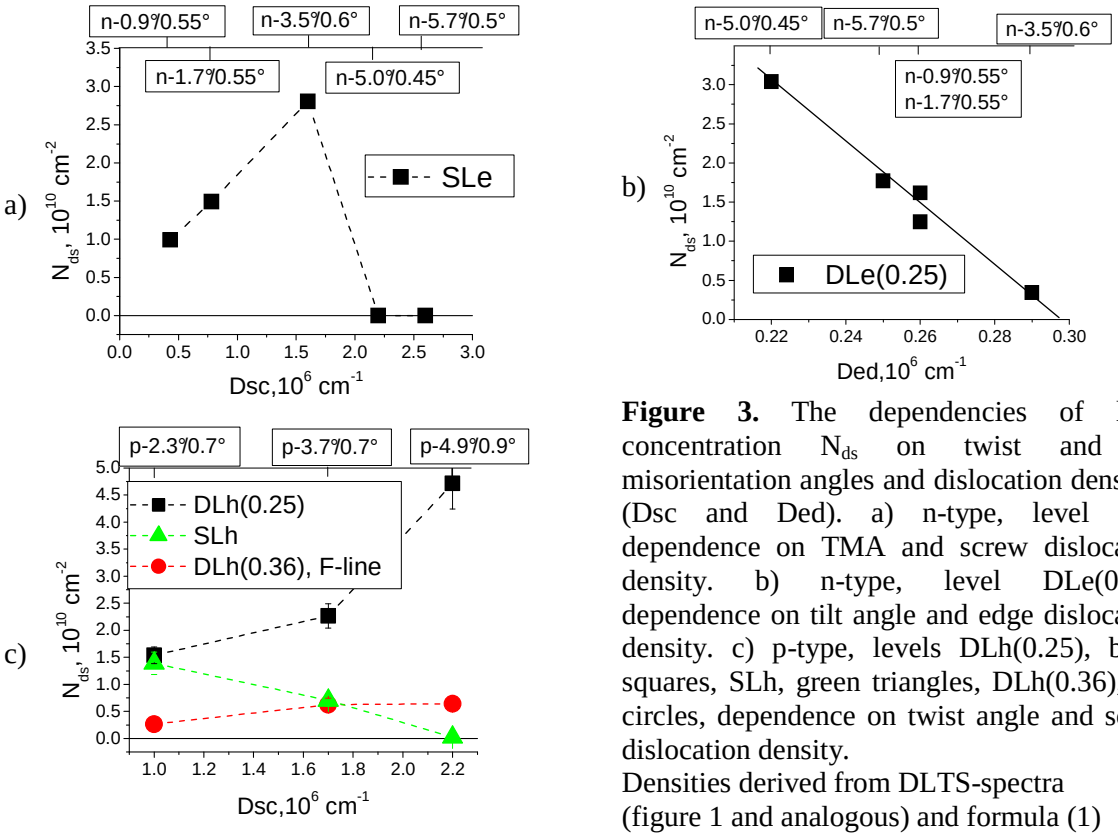

Figure 3. The dependencies of level concentration N_{ds} on twist and tilt misorientation angles and dislocation densities (Dsc and Ded). a) n-type, level SLe, dependence on TMA and screw dislocation density. b) n-type, level DLe(0.25), dependence on tilt angle and edge dislocation density. c) p-type, levels DLh(0.25), black squares, SLh, green triangles, DLh(0.36), red circles, dependence on twist angle and screw dislocation density.
Densities derived from DLTS-spectra (figure 1 and analogous) and formula (1)

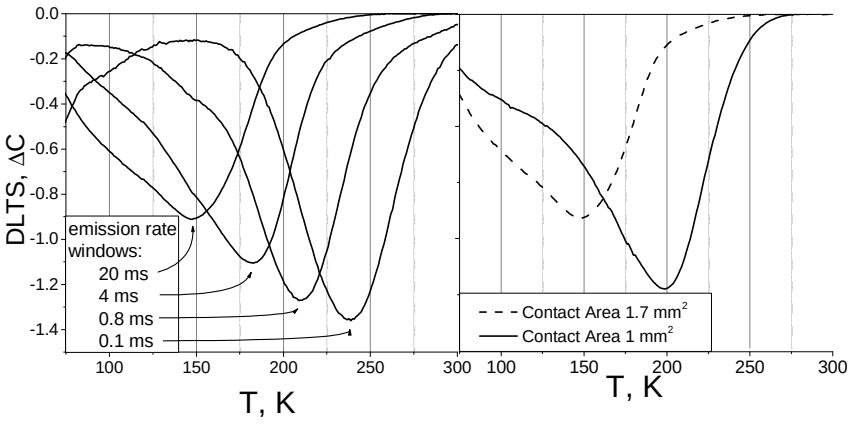

Figure 4. DLTS spectrum of n-2 sample. Typical behaviour of DLe(0.13-0.18) line. Left: peak intensity dependence on emission rate window. Right: peak position dependence on contact area (emission rate window $0.8ms$). DLTS conditions:

$V_{rev} = -1V;\ V_{pulse} = +2V;$
$t_{pulse} = 200\mu s;$
$T_{period} = 50ms$

Secondly, the level DLe(0.25) is observed in all n-type samples. Whereas its concentration has no correlation with TMA it increases with decrease of the tilt misorientation angle, or with the decrease of the edge-type dislocation density (see figure 3b). This proves the 60°-dislocation related origin of level DLe(0.25).

Thirdly, level DLe(0.13-0.18) also observed in all the n-type samples shows peculiar behaviour. This trap has an unexpectedly small cross-section of about 10^{-21} cm^2 with activation energy of 0.15 eV. The DLTS-peak is shifted towards higher temperatures after reducing the area of contact (figure 4 right). The magnitude of the DLTS-peak is increasing with smaller rate window (figure 4 left). Our tentative explanation for these phenomena is as follows: the DLe(0.13-0.18) peak represents a transition between a deep level and a 1D shallow band. The charge thermally emitted from the deep level is in some way trapped on the 1D-band and could be captured by the same deep level or diffuse away from the contact via the conducting channel of the 1D-band. These mechanisms could cause the small cross-section due to much smaller carrier concentration in the 1D-band in comparison with the conduction band, and the dependence on area due to stronger diffusion in the DN plane. The same behaviour of traps was reported in [11] in SiGe quantum wells and explained by lateral diffusion. No correlation between DLe(0.13-0.18) line intensity and twist or tilt misorientation angle was found.

For electron traps there are no direct coincidence with electron levels observed by both Omling [5] ("A","B","C","D" in figure 2a) deep in the band.

n- and p-type samples with similar twist and tilt misorientation angles of ~3.6° and 0.6° respectively were studied by means of DLTS and MCTS to get congruent and comparable data. Figure 5 shows nearly perfect correspondence between DLTS of n-type and MCTS of p-type samples. Levels SLe(0.08). DLe(0.25) and DLe(0.33) are present in both spectra. For DLe(0.25) and DLe(0.33) the concentration of traps are almost the same for both samples, however the low-temperature peak SLe(0.08) is three times larger in the n-type material. The coincidence of peaks allows us to suggest that these peaks are only DN-related and do not originate from contamination or interaction with doping material.

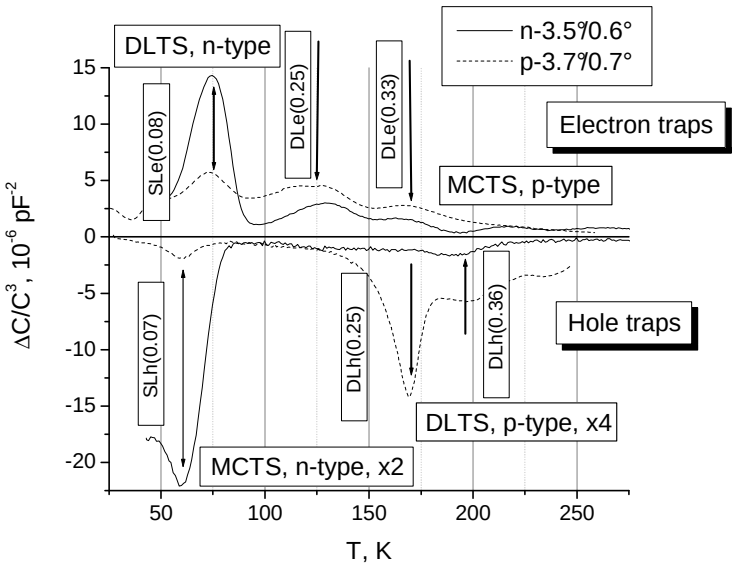

Figure 5. DLTS and MCTS spectra and observed levels for n- and p-type samples with similar misorientation angles of about 3.6°. The corresponding spectra (especially for electrons) coincide with each other well showing the same levels at the same temperatures.

DLTS conditions:
$V_{rev} = -1V;\ V_{pulse} = +2V;$
$t_{pulse} = 200\mu s;\ T_{period} = 50ms,$
emission rate window $0.8ms$.

Figure 1a,b shows DLTS-spectra and corresponding TEM-micrographs to illustrate the dependence of electrical properties of DN on microstructure. While the dislocation network has relatively big cells and pronounced zigzag lines due to interaction between screw and edge dislocations (figure 1a), the most important lines in the spectra are the shallow level SLe and deep level DLe(0.13-0.18). When the

distance between dislocations becomes less than 5 nm and zigzag lines are not visible (figure 1b), the shallow levels disappear whereas the narrow deep levels DLe(0.25) and DLe(0.38) appear.

3.2.2. Levels in the lower half of the band gap in Si

Level SLh(0.07) in p-3.7°/0.7°, n-3.5°/0.6° and n-1.5°/0.55° coincides well with shallow traps for holes in Si observed in [6]. Level SLh(0.09) in p-3.0°/0.7° could be related due to their similar behaviour to SLh(0.07). However, it has intersecting points on the Arrhenius plot and some similar features with the T0-level [6], assigned by the authors to FeB pairs. The concentration of SLh levels in the samples p-2.3°/0.7°, p-3.7°/0.7° and p-4.9°/0.9° (figure 3c) is decreasing with increasing twist misorientation angle or screw dislocation density. This behaviour could be explained by the overlapping strain fields between screw dislocations for higher angle sample, which could in principle result in disappearance of higher energy levels.

The activation energy of level SLh(0.05) observed only in the p-2.3°/0.7° corresponds to the 1D-band energy calculated in [9] for dislocations in p-type Si.

Level DLh(0.25) is observed in all the p-type samples. It corresponds to level "F-dis" observed in [7] and "SD" observed in [12]. The dependence of peak intensity on TMA in samples p-3.7°/0.7°, n-3.5°/0.6°, n-1.5°/0.55° shows the monotonous increase with TMA, *i.e.* with screw dislocation density (figure 3c).

We attribute the DLh(0.36) line, which is also present in all the p-type samples to the F-line first observed by Kimerling and Patel [8]. Investigation of the peak intensities from deconvoluted DLTS-spectra shows that the trap concentration increases with the TMA.

These properties of DLh(0.25) and DLh(0.36) could be due to a number of things: proof of the levels' dependence on screw dislocation line length, intersection points between screw dislocations, or intersection points between screw and edge dislocations. The smaller DLh(0.25) and DLh(0.36) level density in low-angle samples could result in less non-radiative recombination via these levels. This behaviour could increase radiative recombination and thus enhance D1-line intensity.

Similarly to the study of the upper half of the band gap (sec. 3.2.1) we have studied the lower half by comparing corresponding DLTS-spectra of p-type samples and MCTS-spectra of n-type samples (figure 5, Hole traps). The temperature position of SLh(0.07) and DLh(0.36) peaks coincide well. However, the p-type sample exhibits a sharp peak near 170 K which is absent in the n-type sample. This can lead to a suggestion that level DLh(0.25), which is present only in p-type samples (see Table 2), can be a boron-related or processing-related level.

3.3. The Pool-Frenkel effect

The wafer bonding technique introduces dislocations at the interface situated parallel to surface. We assume that charge trapped at the interface doesn't determine the electrical field at the interface. Using Poisson's equation we can derive a simple relation between electrical field and voltage to quantitatively investigate the dependence of DLTS-lines on electrical field:

$$E = eN_d \cdot \left(\frac{S}{C(V)} - \frac{x_d}{\varepsilon\varepsilon_0} \right) - \frac{Q_{ss}}{2\varepsilon\varepsilon_0}, \qquad (3)$$

where e is elementary charge, N_d is the doping concentration, S is the contact area, $C(V)$ is the capacitance dependence on applied voltage, x_d is the interface depth (200nm) and Q_{ss} is the charge trapped on all the deeper levels, calculated from DLTS-spectra using formula (1).

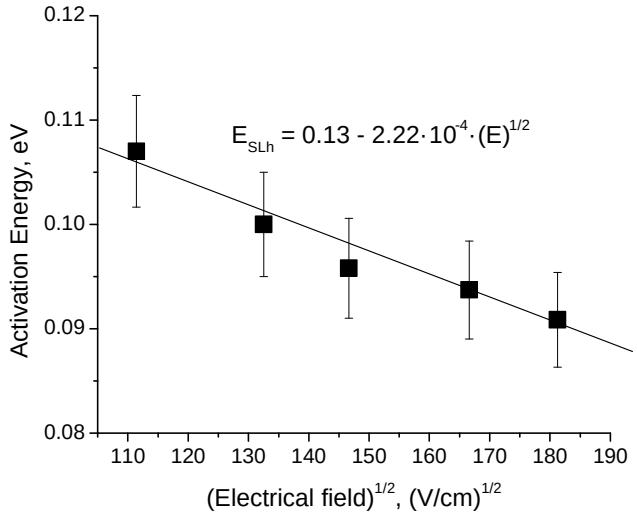

Figure 6. Dependence of level energies on the square root of electrical field. Data measured on sample p-3.0°/0.7°. The Pool-Frenkel effect was observed on level SLh (shallow hole trap, black squares, black solid line represents the linear fitting),

It was reported recently that the SLh-level in analogous samples with TMA = 3° exhibits a Pool-Frenkel shift [12]. The Pool-Frenkel effect was observed only on one of our samples, namely p-3.0°/0.7°. The SLh-level activation energy is plotted versus the square root of electrical field in figure 6. The linear approximation of this data gives the dependence pre-factor of $2.2 \cdot 10^{-4}$ e $V^{1/2}$ $cm^{1/2}$, corresponding well with previously reported data [12]. The extrapolation results in an activation energy of 0.13 eV at zero electrical field. The Pool-Frenkel effect for the shallow electron trap SLe-level was not observed. The absence of the effect might be caused by different reasons: the electrical field was not high enough due to a lower doping level, or the origins of these two shallow levels differ from each other. The absence of Pool-Frenkel effect in similar samples p-3.7°/0.7° and p-2.3°/0.7° could be due to different dislocation microstructure. In fact, all the samples except the p-3.0°/0.7° have tilt axis exactly parallel to [110], or to the screw dislocation line direction (see figure 1). The angle between tilt axis and [110] in sample p-3.0°/0.7° is about 30°. The difference in this angle results in different types of dislocation reactions between 60°- and screw dislocations, which can in turn result in different strain fields around the dislocations. This feature of DN could also cause the difference between DLe(0.25) intensities in p-3.0°/0.7° and p-3.7°/0.7°.

4. Summary

A set of n- and p-type samples with different twist misorientation angles was investigated by means of DLTS, MCTS and TEM measurements. The whole energy band gap in Si was studied. Shallow and deep levels for electrons and holes were found and characterized in all the samples.

The maximum concentration of shallow traps for electrons was found to be in the 3-degrees misoriented sample. The dependencies of activation energy of shallow levels on electrical field were examined. Only one shallow hole trap in one sample (p-3.0°/0.7°) exhibited the Pool-Frenkel effect.

The levels that might have impact on the D1-luminescence are: SLe and SLh which could be a direct source for transition leading to D1-line luminescence, and levels DLh(0.25) and DLh(0.36) which could be active non-radiative centers reducing the amount of direct SLe to SLh transitions. These assumptions will be verified in forthcoming experiments.

We have found that microstructure and self-arrangement of dislocations can dramatically affect electrical properties of the material. The dislocation density derived from twist and tilt misorientation angles is not sufficient to know the exact properties of DN. The difference in the interaction type between 60° and screw dislocations should be examined. The zigzag lines of 60°-dislocations, the angle between rows of tilt dislocations, square meshes of screw dislocations, and probably other

interactions between them can lead to some crucial changes in the electrical and optical properties of the DN.

Acknowledgements
Experimental data presented in this work were obtained using the equipment of Interdisciplinary Resource Center for Nanotechnology of St. Petersburg State University, Russia (http://nano.spbu.ru).

This work was partially supported by RFBR (Grants 08-02-00893, 10-02-01010).

References

[1] Mchedlidze T, Kononchuk O, Arguirov T, Trushin M, Reiche M and Kittler M 2010 *Sol. State. Phenomena* **156-158** 567–572
[2] Kveder V and Kittler M 2008 *Mat. Sc. Forum* **590** 29–56
[3] Ishikawa Y, Yamauchi K, Yamamoto C and Tabe M 2005 *Mater. Res. Soc. Symp. Proc.* **864**
[4] Föll H and Ast D 1979 *Phil. Mag. A* **40** No.5 589–610
[5] Omling P, Weber E R, Montelius L, Alexander H and Michel J 1985 *Phys. Rev. B* **32** 6571
[6] Castaldini A, Cavalcoli D, Cavallini A and Pizzini S 2005 *Phys. Rev. Letters* **95** 076401
[7] Vyvenko O F, Kittler M, Seifert W and Trushin M 2005 *Phys. Stat. Sol. C* **2** No.6 1852-1858
[8] Kimerling L C and Patel J R 1979 *Appl. Phys. Lett*. **34** 73
[9] Farvacque J-L and Franois P 2001 *Phys. Stat. Sol. B* **223** 635–648
[10] Kveder V, Badylevich M, Schröter W, Seibt M, Steinman E and Izotov A 2005 *Phys. Stat. Sol. A* **202** No. 5 901–910
[11] Schmalz K, Yassievich I N, Collart E J and Gravesteijn D J 1996 *Phys. Rev. B* **54** 23
[12] Trushin M, Vyvenko O, Mchedlidze T, Kononchuk O and Kittler M 2010 *Sol. State Phenomena* **156-158** 283-288